CHEMICAL ENGINEERING TRANSACTIONS
VOL. 70, 2018
A publication of AIDIC
The Italian Association of Chemical Engineering
Online at www.aidic.it/cet
Guest Editors: Timothy G. Walmsley, Petar S. Varbanov, Rongxin Su, Jiří J. Klemeš

ISBN 978-88-95608-67-9; **ISSN** 2283-9216
DOI: 10.3303/CET1870254

Comparative Study of Methane Hydrate Formation and Dissociation with Hollow Silica and Activated Carbon

Sarocha Rungrussamee[a], Katipot Inkong[a], Santi Kulprathipanja[b], Pramoch Rangsunvigit[a,*]

[a]The Petroleum and Petrochemical College, Chulalongkorn University, 254 Soi Chulalongkorn 12, Phayathai Rd. Pathumwan, Bangkok 10330, Thailand
[b]UOP, A Honeywell Company, Des Plaines, Illinois, 60017, USA
Pramoch.r@chula.ac.th

Natural gas hydrates are ice-like crystalline compounds and non-stoichiometric, and methane is trapped inside the water cages of the hydrates. In recent years, the hydrates have received much attention for natural gas storage and transportation. However, the use of methane hydrates has faced many challenges such as slow formation rate, low growth rate during hydrate formation, and low conversion ratio of gas to solid hydrates, leading to poor storage capacity. The addition of hydrate promoter is one of alternatives that may overcome these problems. In this work, porous materials, hollow silica (HSC) and activated carbon (AC), were investigated as the hydrate promoters at saturation condition, 1:10 HSC to water and 1:1 AC, to water on the hydrate formation and dissociation. The hydrate formation was conducted in a fix bed reactor at 8 MPa and 4 ºC. The results showed that the methane hydrate formation using the HSC enhanced the water conversion to hydrates and the methane consumption at a greater extent than the methane hydrate formation using the AC. The decomposition of hydrates was performed by thermal stimulation with 21 ºC temperature driving force. The results showed that the porous materials did not significantly affect the methane released and methane recovery from the hydrates.

1. Introduction

Natural gas hydrates are crystalline, ice-like solid composed of gas molecules (guest molecule) trapped with cages formed by water molecules. Solidified Natural Gas (SNG) presents the best option to store natural gas in a large scale with high volumetric storage capacity, 1 m^3 of methane hydrates contains 170 m^3 of methane gas at STP (Englezos and Lee, 2005), not sensitive to the presence of trace hydrocarbon, environmentally friendly, no toxic emission, and non-eruption nature, extremely safe and cost effective (Javanmardi et al., 2005). Natural gas hydrates have attracted much heed as a new means for store and transport natural gas. However, the applications of hydrate storage have been hindered by some problems, for instant, slow kinetics of hydrate formation, interstitial water unreacted, economy of scale up, and the reliability of hydrate storage capacity. Adding promoters can solve that problems by using thermodynamic promoters and kinetic promoters to accelerate the hydrate formation conditions providing one of the flexible and easiest ways to increase the rate of hydrate formation (Sloan and koh, 2007).

In the laboratory, where stirred tank reactors are employed, once the hydrates form, the water conversion to hydrates is low because of the agglomeration of hydrate crystals at the interface (Seo et al., 2014). Effects of additives such as SDS (sodium dodecyl sulfate), APG (alkyl polysaccharide glycoside), and CP (liquid hydrocarbon cyclopenthane) were investigated. SDS was reported to be one of the best additives that can reduce the hydrate induction time and improve hydrate formation rate and storage gas capacity (Sun et al., 2004). Effects of particle size of porous media like activated carbon were also investigated. The experiment with 250 to 420 µm activated carbon showed the fastest methane consumption and methane recovery due to the small particle size had high interconnectivity, which increased the contact area between gas and water, while

Please cite this article as: Rungrussamee S., Inkong K., Kulprathipunja S., Rangsunvigit P., 2018, Comparative study of methane hydrate formation and dissociation with hollow silica and activated carbon , Chemical Engineering Transactions, 70, 1519-1524
DOI:10.3303/CET1870254

the large particle size from 841 to 1680 µm stored the highest methane because it had a large interstitial space and high conversion of water to hydrate (Siangsai et al., 2015). Maize starch was also investigated as a porous media to enhance methane hydrate formation with different concentrations of maize starch on methane hydrate formation and dissociation. It was reported that the high concentration, 800 ppm, increased the formation rate up to 2.5 times compared with no maize starch (Babakhani and Alamdari, 2015). Hollow silica is another porous material with increased attention. Prasad et al. (2014) used hollow silica to enhance methane storage capacity in the gas hydrates. They concluded that the hollow silica structure contained an inner void surrounded by a thinner solid shell. Thus, it could improve the hydrate formation kinetics at a high pressure and low temperature and extremely fast hydrate conversion.
The effects of promoters and porous material was mostly, if not all, reported using a stirred reactor. Few reported these effects on an unstirred reactor. Thus, the purpose of this work was to study effects of hollow silica and activated carbon on methane hydrate formation/dissociation in an unstirred reactor.

2. Experimental Procedures

2.1 Chemical

Hollow silica (99.99 % P-type) was purchased from Nanoshell, India. Activated Carbon supported by Carbokarn Co., LTD., Thailand. Deionized water was used for hydrate formation. Methane gas (CH_4, 99.99 %) was obtained from Linde Public Company, Thailand.

2.2 Experimental Apparatus

The schematic and cross section of gas hydrate apparatus were shown in Figure 1; the system consisted of a high pressure stainless steel crystallizer (CR), a reservoir (R), and a crystallizer. The reservoir was immersed in a cooling bath, the temperature of which was adjusted and controlled by an external controllable circulator. The pressure transducers were used to measure the pressure. The temperature in the crystallizer was measured by using k-type thermocouples (Siangsai et al., 2015). Figure 1 shows the cross section of crystallizer, where the thermocouples were located: T1 at the top of the bed, T2 at the middle of the bed, T3 at the bottom of the bed, and T4 at the bottom of the crystallizer. The pressure and temperature profiles were obtained by using a data logger (AI210 Model, Wisco Industrial instruments, Thailand).

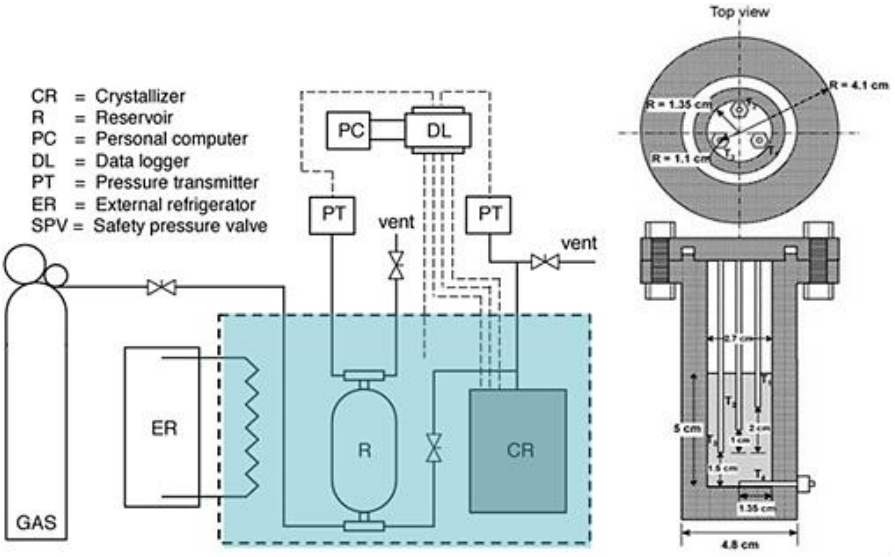

Figure 1: Schematic of experimental apparatus (left side) and cross-section of a crystallizer (right side)

2.3 Methane Hydrate Formation and Dissociation

The porous materials and water were placed in the crystallizer. The crystallizer was cooled until the temperature stabilized. After that, the methane gas was introduced into the system to 0.5 MPa three times to ensure that no air bubble remained in the system. Methane gas was introduced into the crystallizer at the desired experimental condition (8 MPa at 4 °C). The data was then recorded every 10 seconds. Pressure was reduced during the methane formation. The experiment was stopped when there was no significant change in the pressure. After the methane hydrate formation experiment, the hydrates were decomposed by thermal stimulation. The

methane gas released from the hydrates was measured by the pressure transducer. The methane consumption, water conversion, and methane recovery were calculated based on the method outlined Siangsai et al. (2015).

3. Results and Discussion

3.1 Methane Hydrate Formation

The gas uptake and temperature profiles during the hydrate formation with the porous materials at 8 MPa and 4 ºC are shown in Figures 2 and 3, due to the formation of gas hydrates is an exothermic process, so it can be noticed by the temperature spikes of thermocouples in the crystallizer. The induction time used in this context means the interval between the establishment of super saturation and the formation critical nuclei as defined by Khurana et al. (2017). As seen in Figure 2, after the methane gas is introduced to the system, the gas consumption during the hydrate formation can be defined into three stages. The first stage includes the methane gas dissolving into the liquid phase corresponding to the increase in a small amount of gas uptake and pressure drop in the system. In the second stage, when the pressure and temperature are thermodynamically feasible, the hydrates are formed. Then, the hydrates grow with the rapid increase in the gas uptake, which is indicated by the temperature spikes. The temperature of the thermocouples in the crystallizer rises at T1 first, indicating that the hydrate formation with the presence of both the AC and HSC takes place from the top of the bed, which is close to the gas and water interface, and grows to the other locations. Finally, the gas uptake reaches to the optimum and end of the hydrate formation. It is possible that the hydrates initially form at the gas/liquid interface at the crystallizer side wall and grow upwards until the upper edge. At the same time, the water level is decreased due to the water is delivered to grow the methane hydrates. After that, the methane hydrates grow downward into the aqueous phase, which was also reported by Veluswamy et al. (2016b). The physical properties of the HSC is 2.4 $m^2 \cdot g^{-1}$ S_{BET} and 0.1 $g \cdot cm^{-3}$ bulk density (Prasad, 2015), and the AC is 877 $m^2 \cdot g^{-1}$ S_{BET} and pore diameter 2.19 nm (Siangsai et al. 2015), which affects the contact area of gas and liquid interface, the movement of water by capillary force, and the location of hydrates formed above or below the bed (Veluswamy et al. 2016a). From Figure 3, the gas uptake increases again, which can be noticed by the slope of the gas uptake and temperature rises, because the hydrate crystals may be cracked, and water molecules could form methane hydrate again (Chari et al. 2013). Because a very low bulk density of HSC, it disperses on water, which could provide multiple nucleations and easy access from gas to water resulted in the high water conversion to hydrate. The results in Table 1 show that the HSC enhances the methane consumption better than the AC due to the particle size of the HSC is smaller than that the AC. The small particle size results in the high interconnectivity, and interstitial spaces, where the majority of hydrates form, and water conversion to hydrates.

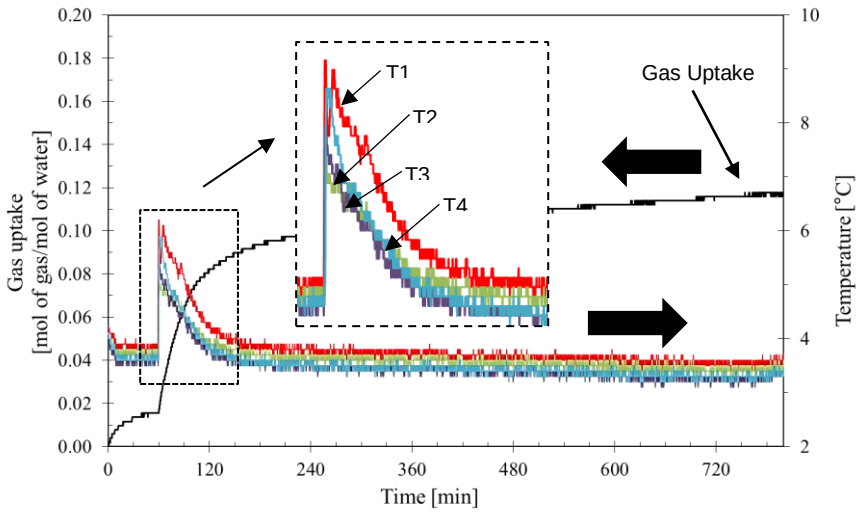

Figure 2: Methane hydrate formation at 8 MPa and 4 °C with the AC

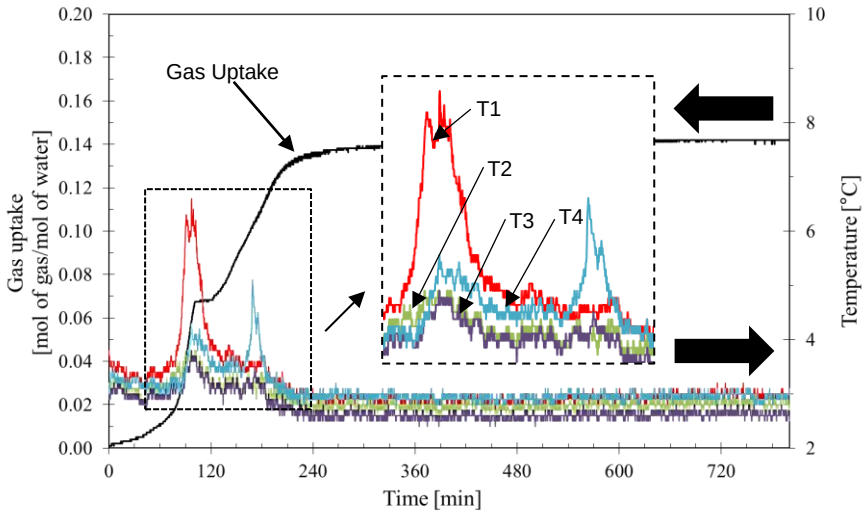

Figure 3: Methane hydrate formation at 8 MPa and 4°C with the HSC

Table 1: Methane hydrate formation experimental condition along with induction time, methane consumed, and water conversion to hydrates with HSC and AC

Exp. No	Induction Time [min]	CH_4 consumed (mol/mole of H_2O)	Water conversion to hydrate (%mol)
HSC			
1	0.50	0.1323	80.56
2	0.17	0.1276	77.71
3	0.17	0.1329	80.92
	Average	0.1309±0.0029	79.73±1.75
AC			
4	0.67	0.0588	67.67
5	0.83	0.0622	67.76
6	0.50	0.0738	66.38
	Average	0.0649±0.0078	67.27±0.77

3.2 Methane Hydrate Dissociation

After the methane hydrate formation process completes, the decomposition starts with thermal stimulation by increasing the temperature from 4 to 25 ºC, temperature driving force 21 ºC. Figures 4 and 5 show methane released and temperature profiles during the dissociation in the presence of porous materials. The temperature in the crystallizer gradually increases by the thermal stimulation and the methane gas was released when the temperature in the crystallizer reaching in free gas zone until it completes. The temperature of the cooling water is set to 25 ºC, causing the heat transfer between the external heater (water) and inside the crystallizer. Therefore, the temperature in the crystallizer is also increased. When the temperature in the crystallizer reaches the dissociation temperature (the first temperature that the methane gas releases) or crosses the hydrate phase equilibrium, the methane gas is released (endothermic reaction). The amount of methane released depends on the methane consumed in each system. Hence, the methane recovery is used for the comparison purpose. Then, the amount of methane released increases until it completes when the temperature of all thermocouple reaches the set point temperature (25 °C).

The methane released and temperature profiles in the system with the AC and the HSC are quite similar but the time to release the methane gas of each thermocouple in the crystallizer are different. The temperature of thermocouple T3, which shows in Figure 4, and the temperature of thermocouple T1, which shows in Figure 5, take the longest time for dissociation, meaning that the methane hydrates at location near the gas and liquid interface is more stable than the other locations.

Table 2 summarizes the methane hydrate dissociation with porous materials at the temperature driving force (ΔT) of 21 °C. The results in the table show that the porous materials in the system in dissociation experiments do not affect the dissociation temperature, methane released, and methane recovery. Methane cannot be recovered 100 % due to some of the methane gas remains in the water and it is not recovered as reported by Linga et al. (2009).

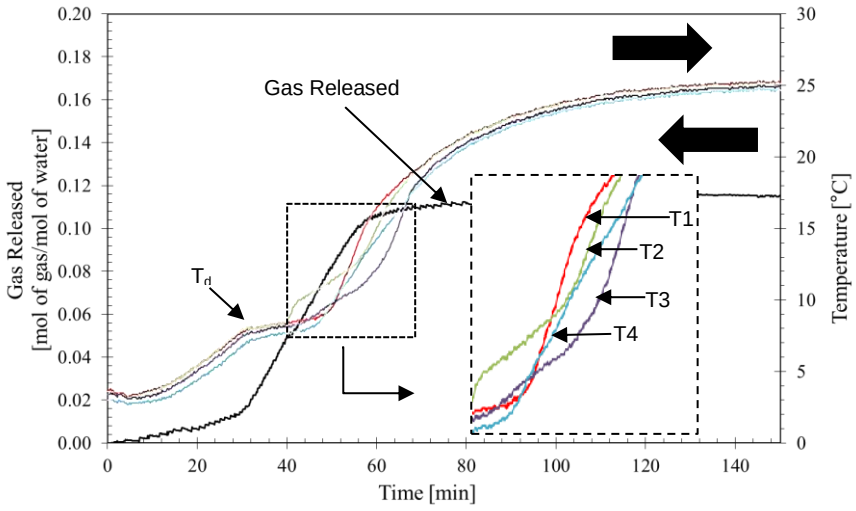

Figure 4: Methane hydrate dissociation with temperature driving force 21 ºC at the saturation of the AC

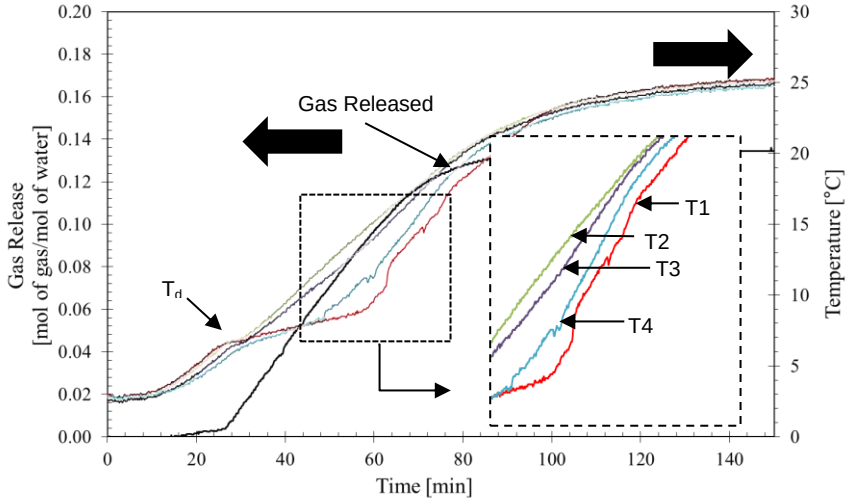

Figure 5: Methane hydrate dissociation with temperature driving force 21 ºC at the saturation of the HSC

Table 2: Methane hydrate dissociation experimental condition along with the dissociation temperature, methane released, and methane recovery in the system with driving force 21 °C

Exp. No	Dissociation Temperature, T_d [°C]	CH_4 Released [mol/mol of H_2O]	CH_4 Recovery [%mol]
HSC			
1	6.6	0.1272	96.11
2	7.0	0.1226	95.14
3	6.6	0.1280	96.32
	Average	0.1259±0.0029	95.86±0.62
AC			
4	7.2	0.0577	98.12
5	7.0	0.0611	98.23
6	7.2	0.0731	99.05
	Average	0.0640±0.0081	98.47±0.51

4. Conclusions

The hollow silica and activated carbon were selected to study for their effects on the methane hydrate formation and dissociation. This study found that the methane hydrate can form in both porous media. The effects of different porous materials with the saturation water condition on the methane hydrate formation were investigated at 8 MPa and 4 ºC in the quiescent condition. The results showed that the presence of the HSC resulted in the methane consumption higher than that with the AC because the AC had a small pore diameter and large particle size resulting in the low interconnectivity space and low water conversion to hydrates. For the methane hydrate dissociation with temperature driving force 21 ºC, even the temperature profiles in the system of AC/H_2O/CH_4 and the system of HS/H_2O/CH_4 were different but the final methane released, and final methane recovery were not significantly different. Therefore, it can be concluded that the types of porous materials could play an important role on the methane hydrate formation at 8 MPa and 4 ºC.

Acknowledgments

The authors would like to sincerely thank the 90th Anniversary of Chulalongkorn University Fund and Grant for International Integration: Chula Research Scholar, Ratchadaphiseksomphot Endowment Fund, Chulalongkorn University, The Petroleum and Petrochemical College, Chulalongkorn University, Thailand; Center of Excellence on Petrochemical and Materials Technology, Thailand; and UOP, A Honeywell Company, USA, for providing support for this research work.

References

Babakhani S.M., Alamdari A., 2015, Effect of maize starch on methane hydrate formation/dissociation rates and stability, Journal of Natural Gas Science and Engineering, 26(8), 1-5.

Chari V.D., Sharma D.V.S.G.K., Prasad P.S.R., Murthy S.R., 2013, Methane hydrates formation and dissociation in nano silica suspension, Journal of Natural Gas Science and Engineering, 11, 7-11.

Englezos P., Lee J.D., 2005, A cleaner source of energy and opportunity for innovative technologies. Department of Chemical & Biological Engineering, The University of British Columbia, 22(5), 671-681.

Javanmardi J., Nasrifar KH., Najibi S.H., Moshfeghian M., 2005, Economic evaluation of natural gas hydrate as an alternative for natural gas transportation, Applied Thermal Engineering, 25, 1708-1723.

Khurana M., Yin, Z., Linga P., 2017, A review of clathrate hydrate nucleation, American Chemical Society, 5, 11176-11203.

Linga P., Haligva C., Nam S.C., Ripmeester J.A., Englezos P., 2009, Gas hydrate formation in a variable volume bed of silica sand particles, Energy and Fuels, 23, 5496-5507.

Prasad P.S.R., Sowjanya Y., Chari V.D., 2014, Enhancement in methane storage capacity in gas hydrates formed in hollow silica, The Journal of Physical Chemistry C, 118, 7759-7764.

Prasad P.S.R., 2015, Methane hydrate formation and dissociation in the presence of hollow silica, The Journal of Chemical Engineering Data, 60, 304-310.

Seo Y., Shin K., Kim H., Wood C.D., Tian W., Kozielski A.K., 2014, Preventing gas hydrate agglomeration with polymer hydrogels, Energy and Fuels, 4409-4420.

Siangsai A., Rangsunvigit P., Kitiyanan B., Kulprathipanja S., Linga P., 2015, Investigation on the roles of activated carbon particle sizes on methane hydrate formation and dissociation, Chemical Engineering Science, 126, 383-389.

Sloan E.D., Koh C.A., 2007, Clathrate hydrates of natural gases, Third Edition, California: CRC press, Prague, Czech Republic.

Sun Z., Ma R., Fan S., Guo K., Wang R., 2004. Investigation on gas storage in methane hydrate, Journal of Natural Gas Chemistry, 13, 107-112.

Veluswamy H.P., Prasad P.S.R., Linga P., 2016a, Mechanism of methane hydrate formation in the presence of hollow silica, Chemical Engineering Journal, 33, 2050-2062.

Veluswamy H.P., Wong A.J.H., Babu P., Kumar R., Kulprathipanja S., Rangsunvigit P., Linga P., 2016b, Rapid methane hydrate formation to develop a cost effective large scale energy storage system, Chemical Engineering Journal, 290, 161-173.